An ARNICA Progress Report

L. K. Hunt & F. Mannucci
C. A. I. S. M. I. - C. N. R.
Largo E. Fermi 5, I-50125 Firenze, Italy
Electronic mail: hunt@arcetri.astro.it, filippo@arcetri.astro.it

ABSTRACT

This report describes technical results obtained with the Arcetri near-infrared camera, ARNICA, mounted at three different telescopes from 1995 to 1998: TIRGO, the Nordic Optical Telescope, and the Vatican Advanced Technology Telescope. For each telescope, we present estimates of the camera+atmosphere efficiency, point- and extended-source sensitivity, telescope emissivity, and mean atmospheric extinction coefficients. We also use data from January, 1995 to January, 1998 to analyze ARNICA's bad pixels and their change with time.

1. Introduction

More than five years have passed since the Arcetri near-infrared (NIR) camera, ARNICA, was first mounted at TIRGO in 1992 (Lisi et al. 1993, Lisi et al. 1996). During the time that the camera has been in operation, it has acquired more than 60 Gigabytes of data (about half a million frames) and has been mounted at five different telescopes.

Here we present a comparative analysis of data from ARNICA mounted at three different telescopes from 1995 to 1997: 1) the 1.5-m f/20 Gornergrat Infrared Telescope[1] (TIRGO); 2) the 2.56-m f/11 Nordic Optical Telescope[2] (NOT); 3) the 1.8-m f/9.5 Vatican Advanced Technology Telescope[3] (VATT). Technical results from the initial campaigns (1992-1994) at TIRGO and the William Herschel Telescope (WHT) have already been reported in Hunt et al. 1996, and a series of technical reports (Hunt et al. 1994a, 1994b, 1994c). The camera, ARNICA, relies on a NICMOS3 256×256 1–2.5 μm HgCdTe scientific grade array, and provides a 4×4 arcmin FOV with 1 arcsec pixels at TIRGO, and 2×2 arcmin with 0.5 arcsec pixels at VATT and NOT.

In the following we report estimates for system efficiency, sensitivity, emissivity, and mean atmospheric extinction coefficients at the different telescopes. We also analyze ARNICA's bad pixels, and discuss the gradual temporal degradation of the cosmetic quality of the array. The latest bad pixel mask is derived from ARNICA observations obtained in January, 1998.

2. Methods and results

We have analyzed ARNICA data for 23 photometric nights, most of which are included in the database for the ARNICA Standard Star Network (Hunt et al. 1998). Table 1 lists the diameters and pixel scales of the three telescopes considered here. Sensitivity calculations, flux conversions, and filter characteristics are as given in Hunt et al. 1994b)[4]. The only exception is that here point-source limiting magnitudes for a given night are derived using an effective aperture defined by 4 times the Gaussian σ (1.7 × FWHM) of the median point-spread function (PSF) measured on that night. In all sensitivity estimates, the collecting area is determined from the primary mirror diameter; neither the loss in collecting area from the central hole in the primary nor the secondary mirror obscuration was taken into account. This means that, especially for NOT and VATT, the values in Table 2 are underestimated.

Table 2 reports the results our analysis for the different telescopes, both in terms of nightly variations, and of global site/telescope means, averaged over the various observing campaigns. The various columns report complete nightly medians that typically involve hundreds of frames. The only exception is the VATT campaign for which we have only mean values of the PSF randomly sampled over the run.

2.1. Efficiency, sensitivity, and seeing

The efficiency η is a global value, and takes into account losses from the atmosphere, the telescope, and the camera. The highest efficiencies were measured at VATT, and are probably due to the lower number (two) of reflecting surfaces in the optical train. The efficiencies at NOT and those at TIRGO in the 1996 run are comparable and higher than those measured in the early runs (1992-1994) at TIRGO. The efficiencies in the April, 1997 TIRGO campaign are degraded relative to the year before, and are very slightly lower than the 1994 values; this degradation may be attributable to the need for aluminization which was performed in Summer, 1997.

[1]TIRGO (Gornergrat, Switzerland) is operated by CAISMI-CNR, Arcetri, Firenze.

[2]NOT is operated on the island of La Palma jointly by Denmark, Finland, Norway, Sweden, in the Spanish Observatorio del Roque de los Muchachos of the Instituto de Astrofisica de Canarias.

[3]VATT (Mount Graham, Arizona) is composed of the Alice P. Lennon Telescope and the Thomas J. Bannan Astrophysics Facility, both operated by the University of Arizona (Steward Observatory) and the Vatican Observatory Research Group.

[4]$F_0 =$ 1560, 1030, 645 Jy, in J, H, and K, respectively.
$\lambda =$ 1.25, 1.65, 2.20 μm in J, H, and K, respectively.
$\Delta\lambda =$ 0.3, 0.3, 0.4 mum J, H, and K, respectively.

TABLE 1
CHARACTERISTICS OF TELESCOPE+ARNICA

Telescope	Diameter (m)	f/ number	Pixel (arcsec)
TIRGO	1.50	20	0.966
NOT	2.56	11	0.546
VATT	1.83	9.5	0.45

The point-source sensitivities should scale with telescope diameter in a background-limited regime, if background and seeing are similar. This is clearly not the case for our data set. TIRGO's rather high J- and H-band backgrounds make it relatively inefficient for $1\,\mu$m work, while its low background in K makes it comparable to telescopes with as much as three times its collecting area, *when the seeing is good as in the 1996 run*. NOT and VATT sensitivities scale rather well, except for the K band, where the slightly lower VATT background makes it comparable to NOT even with half its collecting area.

The median seeing FWHM of the 1996 TIRGO campaign is slightly better than 2 arcsec, that is to say roughly 2 pixels; therefore, this value is probably an upper limit, as narrower PSFs than these are difficult to measure with ARNICA's 1-arcsec pixels at TIRGO. The 1997 run at TIRGO suffered from worse seeing (3 arcsec FWHM), and the point-source sensitivities for this period are consequently lower.

The seeing at NOT is typically good at 1.2–1.4 arcsec in K, although occasionally the seeing can be very good; 20-30% of each night was characterized by sub-arcsec FWHMs. VATT data are not as detailed, but the mean seeing at Mt. Graham appears comparable to that of La Palma.

2.2. Telescope emissivity and K-band background

The measurement of telescope+instrument emissivity is given by the ratio of two quantities: 1) the non-atmospheric contribution to the measured background (NAB), and 2) the flux density from a blackbody. Typically, for the blackbody measurement (BB), one observes an unlit dome or the closed mirror covers. The NAB can be derived from a regression of sky versus airmass, if we assume that the true sky background is proportional to atmospheric path length; any atmospheric contribution from a component that does *not* vary with airmass would be attributed to NAB. In theory, the intercept of such a regression is the background at zero airmass, that is to say the emission of the telescope which we assume to be the sole contributor to NAB. This value should also be comparable to the difference of the minimum (presumably at unit airmass) observed sky background and slope of the above regression. If we have measurements at airmasses (am) 1 and 2, then the NAB can be derived with the simpler expression, NAB=[am1 - (am2-am1)]. In all cases, emissivity is therefore NAB/BB. Figure 1 shows the regressions obtained for the three different telescopes, together with the best-fit regression lines.

TIRGO is characterized by a low emissivity, 12%, as expected because of its infrared-optimized design, and is similar to that measured at UKIRT (12.5% for the three telescope reflecting surfaces). Both optical telescopes, on the other hand, have rather high emissivities: 35% (NOT) and 40% (VATT). In all cases, the two methods – or consistency checks – described above (intercept; minimum sky minus the slope) agree to within 1%. The method of simply measuring the two airmasses performed at VATT gives an emissivity of 40%, which is similar to results from the other two methods: 43% and 41%, respectively. We note finally that (for all telescopes) these are lower limits to the emissivity because the blackbody measurement was always performed

Table 2

ARNICA Efficiencies, Sensitivities, and PSF's

Site Date	η J	η H	η K	Extended Source (mag arcsec^{-2})[a] J	H	K	Point Source (mag)[b] J	H	K	Sky (mag arcsec^{-2}) J	H	K	FWHM (arcsec) J	H	K
NOT															
95aug08	0.18	···	0.36	20.5	···	18.0	20.2	···	18.0	16.3	···	11.8	1.51	···	1.21
95aug09	0.18	···	0.36	20.4	···	17.9	20.2	···	18.0	16.2	···	11.8	1.44	···	1.11
95aug10	···	0.38	0.36	···	19.2	17.9	···	18.6	17.4	···	13.7	11.7	···	1.99	1.93
95aug11	0.16	0.37	0.34	20.0	19.2	17.6	20.1	19.3	17.5	15.5	13.7	11.1	1.12	1.09	1.26
MEAN	0.17	0.37	0.35	20.3	19.2	17.8	20.2	19.0	17.7	16.0	13.7	11.6	1.36	1.54	1.38
TIRGO															
96jan16	0.17	0.31	0.33	19.8	18.7	18.3	···	···	···	15.0	12.9	12.6	···	···	···
96jan17	0.16	0.31	0.34	19.6	18.5	18.3	···	···	···	14.5	12.4	12.4	···	···	···
96jan18	0.18	0.32	0.34	19.7	18.5	18.3	···	···	···	14.7	12.5	12.5	···	···	···
96jan19	0.17	0.33	0.34	19.7	18.6	18.4	18.6	17.4	17.4	14.8	12.6	12.6	1.89	2.05	1.74
96jan20	0.18	0.33	0.34	19.7	18.6	18.4	18.6	17.6	17.5	14.7	12.7	12.7	1.87	1.73	1.61
96jan21	0.18	0.33	0.34	19.3	18.7	18.4	18.1	17.6	17.3	13.9	12.8	12.6	2.12	1.87	1.86
MEAN	0.17	0.32	0.34	19.6	18.6	18.3	18.4	17.6	17.4	14.6	12.7	12.6	1.96	1.88	1.74
NOT															
96aug31	0.18	0.34	0.32	20.1	19.2	17.8	···	···	···	15.6	13.9	11.7	···	···	···
96sep01	0.19	0.34	0.33	20.2	19.2	17.8	20.1	19.0	17.7	15.8	13.8	11.7	1.43	1.40	1.39
96sep02	0.18	0.33	0.33	20.2	19.1	17.8	20.2	19.0	17.7	15.8	13.8	11.7	1.20	1.43	1.45
96sep03	0.18	0.34	0.33	20.4	19.3	17.9	20.0	19.1	17.6	16.1	14.0	11.7	1.65	1.49	1.57
96sep04	0.17	0.33	0.32	20.3	19.3	17.9	20.1	19.4	17.6	16.1	14.1	11.9	1.50	1.08	1.59
MEAN	0.18	0.34	0.33	20.3	19.2	17.9	20.1	19.1	17.6	15.9	13.9	11.7	1.44	1.35	1.50
VATT															
96dec15	0.25	0.42	0.40	19.7	18.5	17.4	19.6	18.5	17.4	15.5	13.4	11.8	1.60	1.44	1.46
96dec16	0.24	0.40	0.39	19.7	18.5	17.5	19.6	18.5	17.5	15.6	13.4	12.0	1.60	1.44	1.46
96dec17	0.23	0.40	0.39	19.8	18.4	17.3	19.7	18.4	17.3	15.8	13.3	11.6	1.60	1.44	1.46
96dec18	0.25	0.40	0.40	19.8	18.2	17.5	19.7	18.2	17.5	15.7	12.8	12.0	1.60	1.44	1.46
96dec20	0.24	0.42	0.40	19.8	18.6	17.6	19.7	18.7	17.6	15.8	13.7	12.1	1.60	1.44	1.46
MEAN	0.24	0.41	0.40	19.7	18.5	17.5	19.6	18.5	17.5	15.7	13.3	11.9	1.60	1.44	1.46
TIRGO															
97apr13	0.13	0.26	0.30	19.7	18.7	18.3	18.0	17.1	16.7	15.0	13.0	12.6	3.21	2.89	3.02
97apr14	0.13	0.27	0.29	19.9	18.9	18.4	18.7	17.7	17.0	15.6	13.5	12.8	2.10	2.19	2.36
97apr15	0.13	0.26	0.29	19.8	18.9	18.3	17.9	17.1	16.8	15.3	13.4	12.6	3.86	3.34	2.80
MEAN	0.13	0.26	0.29	19.8	18.8	18.3	18.2	17.3	16.8	15.3	13.3	12.7	3.06	2.81	2.73

[a] Calculated at 3 σ, in 60 sec.

[b] As a, and assuming a virtual aperture of 1.7 FWHM (Cols. 14–16).

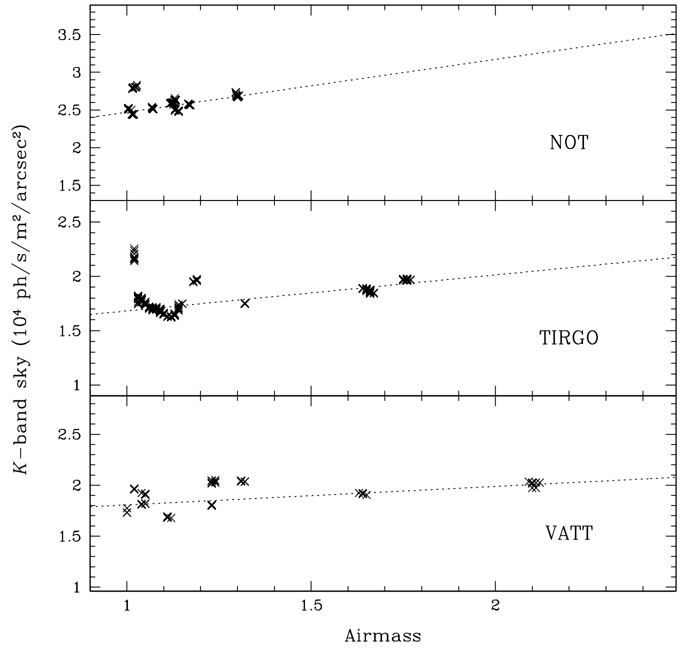

Fig. 1.— Observed K-band background surface brightness (image median) versus airmass. The background surface brightness is given in ph/s/m^2/arcsec^2. The data are from the night when emissivity was measured, and the dotted lines show the best-fit regression described in the text.

at the beginning of the night, when the ambient temperature is presumably warmer than it is later in the night.

Our estimate of the non-atmospheric background at NOT (1.77×10^4 ph/s/m^2/arcsec^2) is similar to that at VATT (1.84×10^4) but slightly higher than that at TIRGO (1.35×10^4). The higher levels are almost certainly due to similarly high telescope emissivity, although the temperatures on the two runs were somewhat different (+8C at NOT, −7C at VATT). The pure sky background emission (at unit airmass) ranges from 0.2×10^4 to 0.7×10^4, with the lowest value at VATT and the highest at NOT. Emission from OH molecules is thought to be the dominant component of NIR airglow up to 2.3 μm (Oliva & Origlia 1992), and indeed non-thermal models of NIR airglow approximate reasonably well the observed spectra (McCaughrean 1988). Such emission originates at 90 km above the Earth's surface, so the different values should not reflect altitude dependence; they more likely reflect the night-to-night or site-to-site variations in the local OH properties.

Finally, we note that the *atmospheric* contribution to the observed background is estimated to be 28% at NOT, 20% at TIRGO, and 9% at VATT. Clearly, the observed K-band background at VATT is dominated by the telescope emission. For a zero-emissivity telescope at the Gornergrat or Mt. Graham, we derive a background emission of around 14.4–14.5 mag/arcsec^2, with a brighter 13.1 mag/arcsec^2 at La Palma for our nights.

2.3. Atmospheric extinction coefficients

Atmostpheric extinction in each band was measured by combining all the nights in a given observing run, and assuming that the extinction is constant from night to night, but that the zero point at unit airmass varies. For an observation of the $j^{\rm th}$ calibrating star on the $i^{\rm th}$ night, we have: $ZP^{obs}_{(i,j)} = ZP^{am=1}_{(i,j)} + k\,(am\,-\,1)$. For each run in each band, we performed a simultaneous fit over the n nights of k and the n values of $ZP^{am=1}_i$. A few of these fits are shown in Fig. 2, and Table 3 gives the extinction coefficients for the various runs at

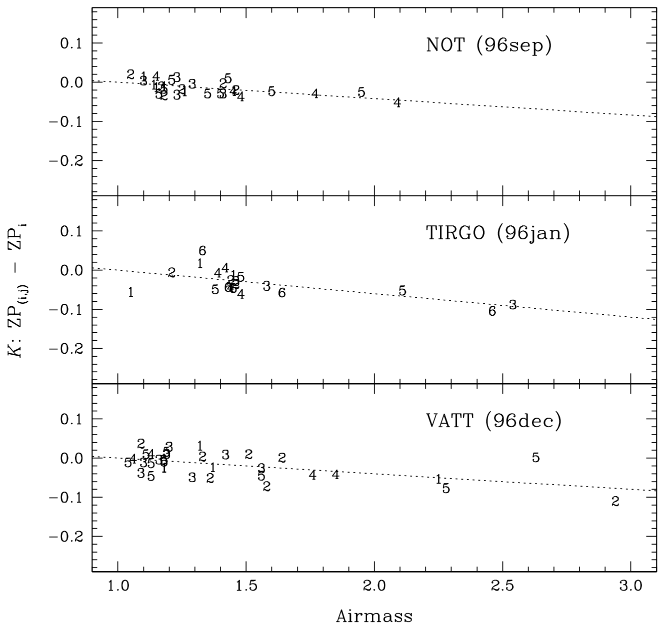

Fig. 2.— K-band $ZP_{(i,j)} - ZP_i$ vs. airmass. Data point are given by the night number (i), and the dotted lines show the best-fit regressions described in the text. The values of the slopes are given in Table 3.

the different telescopes. Results from early ARNICA commissioning runs (1992-1993) and mean photometer values (Hunt et al. 1987) are also included in the table.

Table 3 shows that, although the K-band sky emission is substantially higher at La Palma than at Mt. Graham or the Gornergrat, its extinction properties are similar: the attenuation of zero point with airmass is, on average, -0.04 mag/airmass in K at all sites.

3. Bad pixels

An operational definition of a bad pixel (bp) is a subject of controversy. Some consider bad pixels those which "stand out" in a direct image, that is pixels whose count levels differ significantly from their neighbors; others consider bad pixels those which stand out after the flat-field process, or those which do not behave according to theoretical expectations for the noise. Indeed, a complete and rigorous analysis of the bad pixel behavior in hybrid NIR arrays would be the subject of at least a paper, and perhaps a series of them. Nevertheless, for convenience, we adopt here the former definition of a bp: bp's are singled out by their anomalous behavior relative to the pixels in the neighborhood in the raw images. The definition of "neighborhood" should be such that clearly anomalous clusters of bad pixels are distinguished by the "good" pixels surrounding them.

We used a procedure similar to that described in Hunt et al. (1994c), in which the original high signal-to-noise image is median smoothed, subtracted from the original, and the difference image histogrammed. The histogram is then clipped until it approximates a symmetric distribution with no outliers; the clipped pixels are defined as "bad" and inserted into the bp mask for that date. One difference in the current procedure with respect to 1993 is that now the initial smoothing window had to be larger (10 as opposed to 5 pixels) because of the growth of bp pixel clusters (in particular between 1995 and 1996). Also, the process now needs to be iterated as, because of the larger smoothing window, one pass frequently fails to detect all the bp's that degrade the histogram of the difference

TABLE 3
EXTINCTION COEFFICIENTS

Site	Date	No. Nights	k_J[a]	k_H[a]	k_K[a]
TIRGO	1992 December	8	-0.066 (0.034)	-0.061 (0.035)	-0.053 (0.039)
	1993 February	4	-0.131 (0.057)	-0.048 (0.040)	-0.021 (0.050)
	1996 January	6	-0.042 (0.023)	-0.006 (0.015)	-0.060 (0.029)
	1997 April	3	-0.092 (0.033)	0.000 (0.022)	-0.117 (0.040)
	MEAN	21	-0.083 (0.038)	-0.029 (0.030)	-0.063 (0.040)
TIRGO	1986-1987[b]	5	-0.126 (0.040)	-0.060 (0.019)	-0.076 (0.026)
NOT	1996 September	5	-0.057 (0.022)	0.000 (0.014)	-0.042 (0.019)
VATT	1996 December	5	-0.067 (0.020)	-0.007 (0.012)	-0.040 (0.014)

[a]Units are mag airmass^{-1}. Errors are given in parentheses.

[b]Mean photometer values taken from Hunt et al. 1987. Standard deviations are given in parentheses.

image. When we had more than one image available, masks were determined from each image and compared, and final masks were those which successfully eliminated *all* bp's in all of the images from that date.

We have analyzed mask data from January, 1995, to January, 1998, for a total of five data sets. The 97sep24 mask was acquired by G. Comoretto and R. Maiolino, and the 98jan24 mask by P. Ranfagni, and both were kindly made available to us. The results of the bp selection procedure are given numerically in Table 4. These can be compared with values from June, 1993 (in which the regions are not made contiguous for interpolation), also given in the table.

Generally speaking, the cosmetic quality of ARNICA has degraded slightly from 0.9% in 1993 to 1.2% (Col. 3) five years later; nevertheless ARNICA's array is still in reasonably good shape. We note however several potentially puzzling points that have emerged from our analysis, and then examine each in detail:

1. The bad pixel list does not grow monotonically with time, and not all pixels in an earlier list are contained in the subsequent one.

2. The number of bad pixels defined from a given image depends (in four of five cases) on the count level; the higher the level, the fewer the bad pixels.

3. Two bad columns (128), (256) are clearly present in only two of the five mask images, and their presence does not depend on count level or other parameters that we know of.

4. The latest two images (97sep, 98jan) exhibit double-peaked histograms (when the smoothed image is subtracted as described above) that seem to depend on specific quadrants and whose characteristics change with count level.

One would logically assume that previous bad pixel lists should be subsets of later ones, and that the true detector bad pixels should increase with time. Such assumptions are not warranted in the data we have analyzed here. First, inspection of Table 4 (either Col. 2 or 3) shows that the number of bp's decreases between 95jan and 95nov. This is almost certainly due to the increase of the offset level of the ADCs (analog-digital converters) outside of ARNICA's cryostat that was performed on 11mar95.

Table 4
Bad Pixel Counts

Date	Number	Number w/o 128,256 [a]	Count levels, comments
1993 Jun	580	—	
1995 Jan 05	599	598	5900, 7800; low S/N.
1995 Nov 29	471	470	1900, 4000; vignetting left side.
1996 Nov 20	931	703	1500, 2500, 3500
1997 Sep 24	793	740	3000
1998 Jan 24	1203	764	700, 1400, 2050

[a]Not considering the bad columns 128, 256.

Second, the fraction of pixels in an earlier mask contained in a later one varies between 85 and 95%. This implies either that the procedure to glean bp's from direct images is only 85–95% reliable, or that 5–15% of the pixels defined as "bad"are only sporadically so, and depend on the conditions of the electronics in that moment. We would argue that the latter effect is dominant because: 1) the number of bp's gleaned from different images with the same count levels acquired on the same day are the same to within one or two pixels (< 0.3%); and 2) different bad pixel selection algorithms detect similar sporadic behavior. There is also clear evidence for an electronic origin of some bad pixels, as mentioned in the previous paragraph.

That some bp's can be sporadic is corroborated by the finding that the number of bp's gleaned from a given image depends on count level, an effect also noted in early 1992-1993 data. The change in number of bp's between count levels of 2000 and 4000 is roughly 25–30 pixels; this change was verified on two different dates for which we had more than one image available. For count levels between 700 and 1400, the number changes by 150 or so pixels, although we have only one date with these low flux levels. That the behavior of ARNICA's electronics influences the bp's is also suggested by the sporadic presence of the "bad columns" 128, 256; when they appear, they seem to do so independently of flux levels, and independently of any known effect.

Finally, the most recent images used to derive the bp mask show a histogram (of the original and smoothed image subtraction) with two peaks: a main peak around zero as expected, and a secondary peak towards negative values. The position of the secondary peak, and the separation and widths of the two maxima depend on the count level. The secondary peak is centered roughly on the negative value of the raw image median (± 50 ADU), i.e., the original value of these bp's was approximately zero. The separation of the two peaks gets larger with count level, as does their width. We have some (weak) evidence that also this behavior is due to the DC level prior to the entrance of the ADCs: half of the array appears to contribute more strongly to the negative peak than the other half.

We conclude therefore that the behavior of ARNICA's bad pixels is due partly to real degradation of the cosmetic quality of the array, and partly to variations in the behavior of the electronics. If we believe the reproducibility of the bad pixel detection algorithm, then we can say that these "sporadic" bad pixels comprise roughly 10% of any given bad pixel list.

4. Concluding remarks

In the five or so years that ARNICA has been in operation, it has proved to be a rugged "workhorse", able to function efficiently in very different observing situations. This was made possible by ARNICA's modular design; by S. Gennari and F.

Lisi who designed and implemented the various optical modules to match the different telescopes (Gennari 1997); by C. Baffa, V. Gavryusev, and E. Giani who adapted ARNICA's data acquisition software to different telescopes and operating environments; and by the organizational and observational efforts of R.M. Stanga and L. Vanzi. We hope that the future five years will be as fruitful with the new NIR instruments as these past five years have been.

REFERENCES

Gennari, S. 1997, Arcetri Observatory Technical Report N. 2/97

Hunt, L.K., Calamai, G., & Oliva, E., 1987, Arcetri Observatory Technical Report N. 5/87

Hunt, L., Maiolino, R., & Moriondo, G., 1994a, Arcetri Observatory Technical Report N. 2/94 (Report I)

Hunt, L.K., Maiolino, R., Moriondo, G. & Testi, L. 1994b, Arcetri Technical Report, N. 3/1994 (Report II)

Hunt, L.K., Testi, L., Borelli, S., Maiolino, R., & Moriondo, G. 1994b, Arcetri Technical Report, N. 4/1994 (Report III)

Hunt, L.K., Lisi, F., Testi, L., Baffa, C., Borelli, S., Maiolino, R., Moriondo, G., & Stanga, R.M. 1996, A&ASS, 115, 181

Hunt, L.K., Mannucci, F., Testi, L., Migliorini, S., Stanga, R.M., Baffa, C., Lisi, F., & Vanzi, L. 1998, AJ, in press

Lisi, F., Baffa, C., & Hunt, L. 1993, "ARNICA: the Arcetri Observatory NICMOS-3 imaging camera", Proceedings of SPIE Technical Conference 1946, Orlando

Lisi, F., Baffa, C., Biliotti, V., Bonaccini, D., Del Vecchio, C., Gennari, S., Hunt, L., Marcucci, G., & Stanga, R.M. 1996, PASP, 108, 364

McCaughrean, M. J. 1988, Ph.D. Thesis, University of Edinburgh

Oliva, E., & Origlia, L. 1992, A&A, 254, 466